

# $K_\beta$ to $K_\alpha$ X-RAY INTENSITY RATIOS AND K TO L SHELL VACANCY TRANSFER PROBABILITIES OF Co, Ni, Cu, AND Zn

*L. F. M. Anand<sup>a,b</sup>, S. B. Gudennavar<sup>a,\*</sup>, S. G. Bubbly<sup>a</sup>, B. R. Kerur<sup>c</sup>*

<sup>a</sup> *Department of Physics, Christ University  
Bengaluru-560029, Karnataka, India*

<sup>b</sup> *Department of Physics, Government First Grade College, K. R. Puram  
Bengaluru-560036, Karnataka, India*

<sup>c</sup> *Department of Physics, Gulbarga University  
Kalaburgi-585106, Karnataka, India*

Received May 17, 2015

The K to L shell total vacancy transfer probabilities of low Z elements Co, Ni, Cu, and Zn are estimated by measuring the  $K_\beta$  to  $K_\alpha$  intensity ratio adopting the  $2\pi$ -geometry. The target elements were excited by 32.86 keV barium K-shell X-rays from a weak  $^{137}\text{Cs}$   $\gamma$ -ray source. The emitted K-shell X-rays were detected using a low-energy HPGe X-ray detector coupled to a 16 k MCA. The measured intensity ratios and the total vacancy transfer probabilities are compared with theoretical results and others' work, establishing a good agreement.

DOI: 10.7868/S0044451015120056

## 1. INTRODUCTION

Precise values of K-shell X-ray intensity ratios and total vacancy transfer probabilities are necessary in various fields such as atomic and nuclear physics, materials science, and forensic sciences [1–3]. Also, accurate values of K-shell X-ray intensity ratios provide better understanding of the electron rearrangement phenomenon in the inner shells due to photoionization and nuclear decay processes like the electron capture and internal conversion processes [4–6]. There has been a large amount of work carried out by several researchers adopting single and double reflection geometries and strong radioactive sources of strength  $10^9$  Bq to excite the target samples. Alternately, Horakeri et al. [7–9] proposed a simple  $2\pi$ -geometrical configuration technique with a weak  $\gamma$ -ray excitation source and measured the K-shell X-ray fluorescence parameters of a few high Z elements and compounds. Further investigation of this method in Refs. [10, 11] showed that it can also be used to measure the K-shell X-ray fluorescence cross sections and the ratio of radiative to non-radiative transition widths in addition to the K-shell

X-ray fluorescence yields of medium Z elements and compounds. Recently, it is shown that the method can also be used to measure K-shell X-ray intensity ratios and vacancy transfer probabilities of elements using high resolution detector [12–15]. In this paper, using a nearly  $2\pi$ -geometry with a weak  $^{137}\text{Cs}$   $\gamma$  source of strength less than  $10^4$  Bq, we report the  $K_\beta/K_\alpha$  X-ray intensity ratios and the K to L shell total vacancy transfer probabilities for Co, Ni, Cu, and Zn targets.

## 2. THEORY

The ionization of an atomic shell/subshell leads to the creation of a vacancy in the inner shell of an atom. The vacancy so created is filled by an electron from higher shells, resulting in the emission of fluorescence K-shell X-rays or Auger electron emission. The total vacancy transfer probability from the K-shell to the  $L_i$  shells of an atom is the sum of radiative vacancy transfer probability  $\eta_{KL_i}(R)$  and the nonradiative vacancy transfer probability  $\eta_{KL_i}(A)$ . The total K to L shell vacancy transfer probability is expressed in terms of the K-shell fluorescence yield  $\omega_K$  and the  $I(K_\beta)/I(K_\alpha)$  intensity ratio as [16]

$$\eta_{KL} = \frac{2 - \omega_K}{1 + I(K_\beta)/I(K_\alpha)}. \quad (1)$$

\*E-mail: shivappa.b.gudennavar@christuniversity.in

By using the fluorescence yield values from the literature and measuring  $K_\beta$  to  $K_\alpha$  X-ray intensity ratios, the total vacancy transfer probability from K to L shell can be estimated. The intensity ratio of the characteristic X-rays of type  $i$  to type  $j$  is determined using the equation

$$\frac{I_{(i)}}{I_{(j)}} = \frac{I'_i \varepsilon_j \beta_j \exp(-\mu_{xjw} t_w)}{I'_j \varepsilon_i \beta_i \exp(-\mu_{xiw} t_w)}, \quad (2)$$

where  $I'_i$  and  $I'_j$  are the measured intensities of K-shell X-rays of types  $i$  and  $j$  ( $i = K_\beta$  and  $j = K_\alpha$ ),  $\varepsilon_i$  and  $\varepsilon_j$  are the efficiencies of the detector for K-shell X-rays of types  $i$  and  $j$ ,  $\beta_i$  and  $\beta_j$  are the self-attenuation correction factors for K-shell X-rays of type  $i$  and type  $j$  in the target material and are calculated using Eq. (3), and  $\exp(-\mu_{xiw} t_w)$  and  $\exp(-\mu_{xjw} t_w)$  are the detector window attenuation correction factors for K-shell X-rays of types  $i$  and  $j$ ; here,  $\mu_{xiw}$  and  $\mu_{xjw}$  are the mass attenuation coefficients ( $\text{cm}^2/\text{g}$ ) of K-shell X-rays of types  $i$  and  $j$  in the detector window of a thickness  $t_w$  ( $\text{g}/\text{cm}^2$ ) and are computed using WinXcom software [17]. Since the emission of K-shell X-rays is isotropic and because we are measuring the intensity of K-shell X-rays transmitted from the target in the forward hemisphere (the characteristic X-ray photons emitted into a solid angle of nearly  $2\pi$  sr), we use the self-attenuation correction factor  $\beta$  that is independent of the scattering angles (for details, we refer the reader to Refs. [7–11]),

$$\beta = \frac{1 - \exp(-(\mu_i + \mu_e)t)}{(\mu_i + \mu_e)t}, \quad (3)$$

where  $t$  is the target thickness ( $\text{g}/\text{cm}^2$ ),  $\mu_i$  and  $\mu_e$  are the mass attenuation coefficients ( $\text{cm}^2/\text{g}$ ) of the incident photons and the emitted K-shell X-ray photons in the target. These coefficients have been computed using the WinXcom software [17]. The thickness of the targets is chosen such that the self-absorption correction factor  $\beta$  falls in the range  $0.75 \leq \beta \leq 0.95$ .

### 3. EXPERIMENTAL

The experimental arrangement is as shown in Fig. 1. In the present work, we have used a  $^{137}\text{Cs}$  gamma source of the strength  $10^4$  Bq as the excitation source.  $^{137}\text{Cs}$  source undergoes  $\beta$  decay leaving the daughter nucleus in a metastable state,  $^{137m}\text{Ba}$ .  $^{137m}\text{Ba}$  decays to its ground state either by emitting a  $\gamma$ -ray of the energy 662 keV or by the internal conversion resulting in the emission of K-shell X-rays of barium with a weighted average energy of 32.86 keV. In the present work, we use 32.86 keV Ba K-shell X-ray photons for exciting the

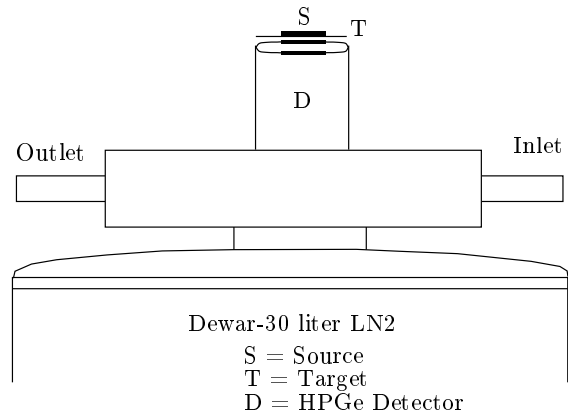


Fig. 1. Experimental arrangement

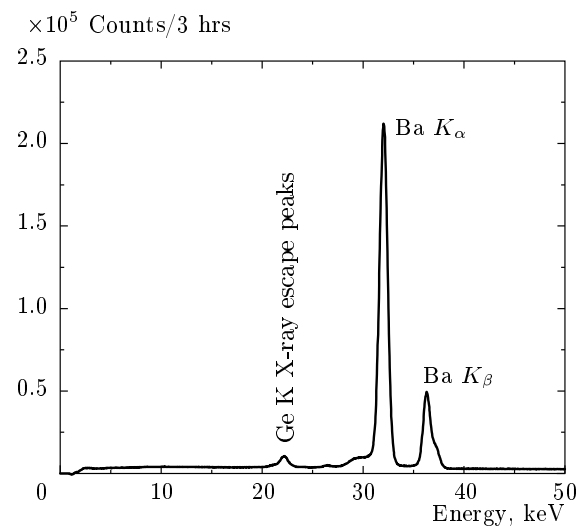


Fig. 2. Source plus background spectrum

low Z elemental targets. We used a low energy HPGe detector with the energy resolution of 200 eV at 5.9 keV and with the absolute efficiency of nearly 100 % in the energy range 3–500 keV. The details of the detector used, specifications, and its dead layer thickness are discussed elsewhere [14]. The targets investigated are pure elements (99.99 %), procured in the form of thin foils of required thickness from Alfa Aesar A Johnson Matthey Company UK.

The intensity of K-shell X-ray photons from the target is measured as follows. The “source with a background spectrum” was acquired by placing the source on the window of the detector (Fig. 2). A live time of 3 hrs was set in the multichannel analyser to obtain the intensity sufficient to minimize the uncertainty in the results due to counting statistics. Then by sandwiching the target between the source and the detector

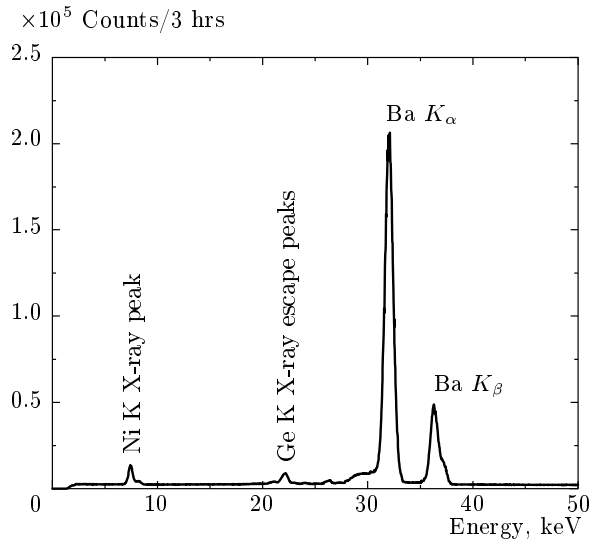


Fig. 3. Transmitted spectrum Ba K X-rays through Ni target

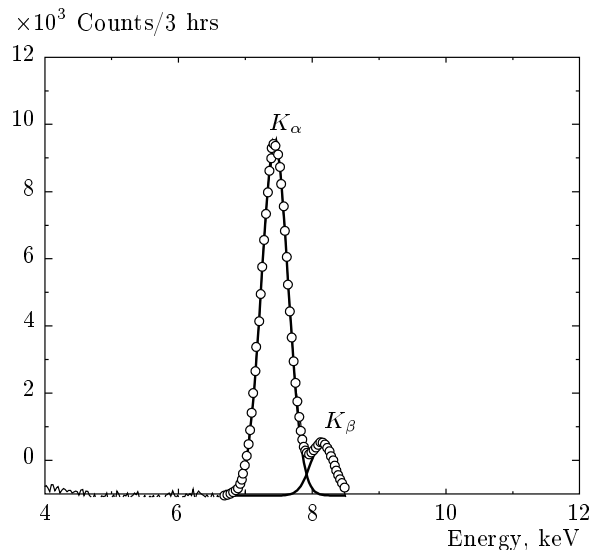


Fig. 4. Fluorescence K-shell X-ray spectrum of Ni

window, the “transmitted spectrum with a background” was acquired for the same interval of time (Fig. 3). The “source with the background spectrum” is carefully subtracted from the “transmitted spectrum with the background” using ORIGIN software. This gives the K-shell X-ray fluorescence spectrum of the target element under investigation (Fig. 4). However, we found that the K-shell X-ray peaks were not fully resolved at its base, as can be seen from Fig. 4. Hence, we have used the ORIGIN multi-peak analysis tool to address this problem and estimated the area under the respective K-shell X-ray peaks. Thus, the K-shell X-ray intensities of the

target elements were determined. They were then corrected for self-attenuation of the emitted K-shell X-rays in the target, the attenuation in the window of the detector, the efficiency of the detector, and the dead layer attenuation. Since there is a gap of 5 mm between the window of the HPGGe detector and its active material, the solid angle subtended by the target at the detector is slightly less than the  $2\pi$  sr solid angle. Hence, by applying the solid angle correction, the total number of K-shell X-rays emitted in the forward hemisphere from the target is estimated. Further multiplying this intensity by 2 gives the total number of K-shell X-rays emitted in the  $4\pi$  sr solid angle. The intensity ratio for the elements under study is calculated using Eq. (2). For the consistency and reproducibility, the experiment was repeated four times for each of the target elements; the weighted average of the four trials is presented in Table 1. From the measured values of the  $I_{K_\beta}/I_{K_\alpha}$  intensity ratios and with the  $\omega_K$  values adopted from the tables in Refs. [18,19], the K to L total vacancy transfer probabilities are evaluated using Eq. (1). The estimated values of K to L total vacancy transfer probabilities for Co, Ni, Cu, and Zn targets along with the associated uncertainties are presented in Table 2.

#### 4. RESULTS AND DISCUSSION

The K-shell X-ray intensity ratios for the low Z elements Co, Ni, Cu, and Zn have been measured using the procedure detailed in the experimental section. The measured value of  $I_{K_\beta}/I_{K_\alpha}$  for these elements and the theoretical values of Rao et al. [20], Scofield [21], Manson and Kennedy [22], and Khan and Karimi [23] and other experimental values obtained by adopting various reflection geometries are presented in Table 1. From Table 1, we see that our results fairly agree with the theoretical and other experimental values for the target elements investigated. The uncertainty in the measured value of the K-shell X-ray intensity ratio is 3.2% for Ni and Zn, and 6.5% for Co and Cu. The uncertainty present in our measured value of  $I_{K_\beta}/I_{K_\alpha}$  for the elements investigated is attributed to uncertainties arising from counting statistics (less than 3%), the target thickness and self-attenuation correction factor (less than 1%), the window attenuation correction (less than 0.1%), and the absolute efficiency of the detector (less than 8%). Our measured data of the K-shell X-ray intensity ratio and the theoretical values in [21] and [22] differ by 2% and by less than 10% from the references in [20] and [23].

**Table 1.** Comparison of  $I_{K_\beta}/I_{K_\alpha}$  values for Co, Ni, Cu, and Zn

Target Elements	Present Work	Theory	Others' Experimental
Co	$0.123 \pm 0.008$	0.1218 [21]	$0.1273 \pm 0.0065$ [1]
		0.1219 [22]	$0.122 \pm 0.006$ [2]
		0.1350 [23]	$0.1322 \pm 0.0012$ [24]
			$0.1207 \pm 0.0062$ [25]
			$0.1390 \pm 0.007$ [26]
			$0.137 \pm 0.011$ [27]
		$0.133 \pm 0.010$ [28]	
Ni	$0.125 \pm 0.004$	0.135 [20]	$0.1283 \pm 0.0065$ [1]
		0.1227 [21]	$0.121 \pm 0.006$ [2]
		0.1221 [22]	$0.1358 \pm 0.0014$ [24]
		0.136 [23]	$0.1210 \pm 0.0062$ [25]
			$0.1330 \pm 0.003$ [26]
			$0.138 \pm 0.011$ [27]
		$0.135 \pm 0.012$ [28]	
Cu	$0.124 \pm 0.009$	0.1216 [21]	$0.1258 \pm 0.0064$ [1]
		0.1208 [22]	$0.120 \pm 0.006$ [2]
		0.137 [23]	$0.1345 \pm 0.0014$ [24]
			$0.1197 \pm 0.0061$ [25]
			$0.1359 \pm 0.003$ [26]
			$0.139 \pm 0.0130$ [27]
		$0.134 \pm 0.013$ [28]	
Zn	$0.127 \pm 0.004$	0.135 [20]	$0.1278 \pm 0.0065$ [1]
		0.1241 [21]	$0.126 \pm 0.006$ [2]
		0.1233 [22]	$0.1245 \pm 0.0034$ [24]
		0.139 [23]	$0.1167 \pm 0.0060$ [25]
			$0.1379 \pm 0.005$ [26]
			$0.141 \pm 0.010$ [27]
		$0.136 \pm 0.010$ [28]	

The estimated total vacancy transfer probability for these elements in our work is compared with the fitted value in [29], theoretical and other experimental works, and presented in Table 2. The uncertainty in the values of  $\eta_{KL}$  is 3.2% to 7.5%. The uncertainty in  $\eta_{KL}$  is a cascade of uncertainties in the  $\omega_K$  and  $I_{K_\beta}/I_{K_\alpha}$  values. A difference of 3% to 10% is present between our estimated values of  $\eta_{KL}$ , and theoretical and other experimental works for all the target elements investigated.

## 5. CONCLUSIONS

Good agreement between the measured and estimated values of K-shell X-ray fluorescence parameters from the present work, and theoretical and others' experimental values shows that the method can be a simple alternative to the measurements of K-shell X-ray intensity ratios of low Z elements. The work also extends a scope for further study of the other X-ray fluorescence parameters for low- and medium-Z elements by this method and its validation. However,

**Table 2.** Comparison of  $\eta_{KL}$  values for Co, Ni, Cu, and Zn

Element	Present*	Present**	Fitted	Theory	Others'
Co	$1.454 \pm 0.098$	$1.435 \pm 0.098$	1.445 [29]	1.418 [16] 1.416 [29]	$1.4169 \pm 0.0723$ [1] $1.420 \pm 0.142$ [30] $1.415 \pm 0.057$ [29] $1.418 \pm 0.011$ [27]
Ni	$1.412 \pm 0.048$	$1.404 \pm 0.042$	1.412 [29]	1.375 [20] 1.388 [16] 1.384 [29]	$1.3853 \pm 0.0707$ [1] $1.364 \pm 0.123$ [30] $1.394 \pm 0.042$ [29] $1.388 \pm 0.011$ [27]
Cu	$1.386 \pm 0.111$	$1.375 \pm 0.105$	1.380 [29]	1.357 [16] 1.354 [29]	$1.3523 \pm 0.0690$ [1] $1.342 \pm 0.121$ [30] $1.361 \pm 0.041$ [29] $1.357 \pm 0.012$ [27]
Zn	$1.352 \pm 0.043$	$1.3439 \pm 0.045$	1.349 [29]	1.316 [20] 1.326 [16] 1.324 [29]	$1.3311 \pm 0.0679$ [1] $1.298 \pm 0.104$ [30] $1.330 \pm 0.040$ [29] $1.327 \pm 0.09$ [27]

\*Calculated taking  $\omega_K$  from Kahoul et al. [18]; \*\*Calculated taking  $\omega_K$  from Hubbell et al. [19]

there are a few difficulties in measuring the K-shell X-ray intensity ratio in the softer spectral band or in the measurement of the K X-ray photons of low energies, namely, the difficulty in resolving the K X-ray peaks in order to estimate their intensities, and overcoming the presence of high background counts in the spectral range of the emitted K X-ray photons. These difficulties could be addressed by using high-resolution detectors.

One of the authors (LFMA) acknowledges partial financial support by the University Grants Commission, New Delhi, India through the minor research project, MRP(S)/2013-14/KABA095/UGC-SWRO.

#### REFERENCES

1. V. Aylikci, A. Kahoul, N. K. Aylikci, E. Tiraşoğlu, and I. H. Karahan, *Spectroscop. Lett.* **48**, 331 (2014).
2. D. Demir and Y. Şahin, *Radiat. Phys. Chem.* **85**, 64 (2013).
3. H. Baltas, B. Ertugral, C. Kantar et al., *Phys. Pol. A* **119**, 764 (2011).
4. I. Han and L. Demir, *Radiat. Phys. Chem.* **79**, 1174 (2010).
5. B. Ertuğral, H. Baltaş, A. Çelik, and Y. Kobya, *Acta. Phys. Pol. A* **117**, 333 (2010).
6. E. Arndt, G. Brunner, and E. Hartmann, *J. Phys. B: At. Mol. Phys.* **15**, 887 (1982).
7. L. D. Horakeri, S. G. Bubbly, and S. B. Gudennavar, *Radiat. Phys. Chem.* **80**, 626 (2011).
8. L. D. Horakeri, B. Hanumaiah, and S. R. Thontadarya, *X-ray Spectrom.* **27**, 344 (1998).
9. L. D. Horakeri, B. Hanumaiah, and S. R. Thontadarya, *X-ray Spectrom.* **26**, 69 (1997).
10. S. B. Gudennavar, N. M. Badiger, S. R. Thontadarya, and B. Hanumaiah, *Radiat. Amer. J. Phys.* **71**, 822 (2003).
11. S. B. Gudennavar, N. M. Badiger, S. R. Thontadarya, and B. Hanumaiah, *Radiat. Phys. Chem.* **68**, 721 (2003b); S. B. Gudennavar, N. M. Badiger, S. R. Thontadarya, and B. Hanumaih, *Radiat. Phys. Chem.* **68**, 745 (2003).
12. A. S. Bennal, K. M. Niranjana, and N. M. Badiger, *J. Quant. Spectr. Rad. Trans.* **111**, 1363 (2010).

13. A. S. Bernal and N. M. Badiger, *J. Phys. B: At. Mol. Opt. Phys.* **40**, 2189 (2007).
14. L. F. M. Anand, S. B. Gudennavar, S. G. Bubbly, and B. R. Kerur, *JETP* **119**, 392 (2014).
15. L. F. M. Anand, S. B. Gudennavar, J. Daisy, and S. G. Bubbly, *Uni. J. Phys. Appl.* **1**, 83 (2013).
16. E. Schönfeld and H. Janßen, *Nucl. Instr. Meth. A* **369**, 527 (1996).
17. M. J. Berger, J. H. Hubbell, S. M. Seltzer et al., *XCOM: Photon Cross Section Database (version 1.3)*, National Institute of Standards and Technology, Gaithersburg MD (2005).
18. A. Kahoul, V. Aylikci, N. K. Aylikci et al., *Radiat. Phys. Chem.* **81**, 713 (2012).
19. J. H. Hubbell, P. N. Trehan, N. Singh et al., *J. Phys. Chem. Ref. Data* **23**, 339 (1994).
20. P. V. Rao, M. H. Chen, and B. Crasemann, *Phys. Rev. A* **15**, 997 (1972).
21. J. H. Scofield, *At. Data Nucl. Data Tables* **14**, 121 (1974).
22. S. T. Manson and D. J. Kennedy, *At. Data Nucl. Data Tables* **14**, 112 (1974).
23. M. R. Khan and M. Karimi, *X-ray Spectrom.* **9**, 32 (1980).
24. A. Kahoul, N. K. Aylikci, V. Aylikci et al., *J. Radiat. Res. Appl. Sci.* **7**, 346 (2014).
25. E. Cengiz, Z. Biyiklioğlu, N. K. Aylikci et al., *Chin. J. Chem. Phys.* **23**, 138 (2010).
26. B. Ertuğural, G. Apaydin, U. Çevik et al., *Radiat. Phys. Chem.* **76**, 15 (2007).
27. Elif Öz, *J. Quant. Spectr. Rad. Trans.* **97**, 41 (2006).
28. M. Ertuğural, Ö. Söğüt, Ö. Şimşek, and E. Büyükkasap, *J. Phys. B* **34**, 909 (2001).
29. B. Ertuğural, G. Apaydin, A. Tekbiyik et al., *Eur. Phys. J. D* **37**, 371 (2006).
30. Ö. Söğüt, E. Büyükkasap, A. Küçükönder, and T. Tarakçioğlu, *Pramana* **73**, 711 (2009).